© 2021. Published by The Company of Biologists Ltd | Journal of Experimental Biology (2021) 224, jeb228221. doi:10.1242/jeb.228221

RESEARCH ARTICLE

Lower-limb muscle function is influenced by changing mechanical demands in cycling

Adrian K. M. Lai[1], Taylor J. M. Dick[2], Nicholas A. T. Brown[3], Andrew A. Biewener[4] and James M. Wakeling[1,*]

ABSTRACT

Although cycling is a seemingly simple, reciprocal task, muscles must adapt their function to satisfy changes in mechanical demands induced by higher crank torques and faster pedalling cadences. We examined whether muscle function was sensitive to these changes in mechanical demands across a wide range of pedalling conditions. We collected experimental data of cycling where crank torque and pedalling cadence were independently varied from 13 to 44 N m and 60 to 140 rpm. These data were used in conjunction with musculoskeletal simulations and a recently developed functional index-based approach to characterise the role of human lower-limb muscles. We found that in muscles that generate most of the mechanical power and work during cycling, greater crank torque induced shifts towards greater muscle activation, greater positive muscle–tendon unit (MTU) work and a more motor-like function, particularly in the limb extensors. Conversely, with faster pedalling cadence, the same muscles exhibited a phase advance in muscle activity prior to crank top dead centre, which led to greater negative MTU power and work and shifted the muscles to contract with more spring-like behaviour. Our results illustrate the capacity for muscles to adapt their function to satisfy the mechanical demands of the task, even during highly constrained reciprocal tasks such as cycling. Understanding how muscles shift their contractile performance under varied mechanical and environmental demands may inform decisions on how to optimise pedalling performance and to design targeted cycling rehabilitation therapies for muscle-specific injuries or deficits.

KEY WORDS: Work, Power, Muscle–tendon unit, Musculoskeletal modelling, Coordination

INTRODUCTION

Skeletal muscles function to generate force and power to produce movement. During movement, muscles have been shown to play a variety of roles to accommodate varying mechanical demands linked to environmental constraints. As such, skeletal muscles can act as ‘motors’, ‘springs’, ‘struts’ or ‘dampers’ in order to mediate differing motor behaviours (Dickinson et al., 2000). For example, the mechanical function of the turkey and guinea fowl gastrocnemius muscle shifts from a relatively isometric (strut-like) behaviour during level running to shortening and performing work (motor-like) during incline running (Daley and Biewener, 2003; Roberts et al., 1997). In contrast, deep, red muscles in yellowfin tuna and the pectoralis muscles in pigeons function exclusively as motors for power production during swimming and flight, respectively (Biewener, 1998; Katz et al., 2001). These animal studies have elegantly demonstrated that it is predominantly the timing of activation and the resultant force production relative to muscle strain that has a considerable effect on muscle function during dynamic tasks (Biewener et al., 2004; Dickinson et al., 2000; Josephson, 1985; Roberts et al., 1997), yet this remains challenging to assess in human experiments because of the invasive techniques required to measure *in vivo* muscle forces.

Musculoskeletal simulations, combined with non-invasive experimental data, provide a promising approach to quantify muscle function during human movement. Recent application of this approach, originally developed to characterise joint function (Qiao and Jindrich, 2016), to human locomotion suggests that during walking and running, proximal muscles in the human lower limb are more motor-like in function compared with distal muscles, which function more like springs and struts (Lai et al., 2019). This approach combined experimental data and musculoskeletal simulations to classify muscles into functional roles enabling quantitative measures of muscle function during dynamic movement. These four functional roles can be defined as (1) ‘motors’ that generate positive work; (2) ‘springs’ that store and recover energy; (3) ‘struts’ that generate significant force with minimal length change; and (4) ‘dampers’ that lengthen to absorb energy.

Human lower limbs perform a variety of locomotor tasks, such as walking, running, cycling, stair climbing, jumping and hopping, which offer the opportunity to explore how human muscles accommodate these varying mechanical demands and environmental constraints. Cycling has been used extensively to study human muscle function because of its highly constrained reciprocal limb extension and flexion phases – similar to human gait. However, cycling differs from human gait because the movement patterns are constrained by contact with the environment via the saddle and pedals (Hull and Jorge, 1985) and because the primary task in cycling is to generate power and perform positive work. Additionally, cycling offers the experimental convenience of varying mechanical demands required to drive the cranks by independently altering the external crank torque or the movement speed (pedalling cadence), all with consistent kinematics, which is challenging to enforce during gait. A deeper understanding of how the function of individual lower-limb muscles varies with torque- and speed-dependent alterations in the mechanical demands of cycling may be important for the optimisation of pedalling performance and the use of cycling as a targeted rehabilitation therapy for muscle-specific injuries or deficits resulting from neuromuscular disorders, such as stroke. In this study, we combined experimental measures of muscle activity, together with musculoskeletal simulations and an index-based

[1]Department of Biomedical Physiology and Kinesiology, Simon Fraser University, Burnaby, BC, Canada, V5A 1S6. [2]School of Biomedical Sciences, University of Queensland, St Lucia, QLD 4072, Australia. [3]Faculty of Health, University of Canberra, Canberra, ACT 2617, Australia. [4]Concord Field Station, Harvard University, Bedford, MA 01730, USA.

*Author for correspondence (james_wakeling@sfu.ca)

A.K.M.L., 0000-0002-8931-0878; T.J.M.D., 0000-0001-8371-6247; J.M.W., 0000-0001-6050-6271

Received 19 May 2020; Accepted 20 December 2020

approach to determine the functional roles of lower-limb muscles when mechanical demands are varied during human cycling.

Cycling research to date has largely focused on the function of single muscles or muscle groups based on the magnitude and timing of muscle activity (for review, see Hug and Dorel, 2009). Studies have shown that differences in the relative magnitude of muscle activity occur in response to varied crank torque and pedalling cadence. In particular, greater muscle activity occurs with increases in both crank torque and cadence, but the relationship between muscle activity and the mechanical demands of the task is muscle specific (Wakeling and Horn, 2009). As pedalling cadence increases, lower-limb muscles activate earlier within the crank cycle, probably because the electromechanical delay of the muscle contraction represents an increasingly greater proportion of the cycle duration at these higher cadences (Neptune et al., 1997; Wakeling and Horn, 2009). There has also been focus placed on the production of positive mechanical work, which is logical given that it is the production of positive power and work that is necessary to propel the rider and bicycle forward (Ericson, 1988). Proximal muscles at the hip and knee have been shown to produce the majority of this positive work (Broker and Gregor, 1994; Martin and Brown, 2009; Martin and Nichols, 2018), suggesting a motor-like function of these proximal muscles. Interestingly, maximal cycling requires more positive power from hip extensor muscles (Martin and Brown, 2009; Martin and Nichols, 2018) compared with submaximal cycling, in which the knee flexors and extensors generate ∼70% of the total positive power (Broker and Gregor, 1994). Despite this, substantial negative mechanical work has been observed during the upstroke phase of cycling (∼190–340 deg), particularly at higher cadences (Neptune and Herzog, 1999; Neptune and van den Bogert, 1997), which may not support the need for the motor-like function of muscles. Instead, a more spring-, strut- or damper-like function may be better suited for higher cadences to accommodate higher segmental acceleration and allow for the transfer of this segmental energy to the cranks as external work (Kautz and Neptune, 2002).

The aim of this study was to determine the mechanical power and work contributions of human lower-limb muscles during cycling and whether these functions are sensitive to changes in the mechanical demands across a wide range of pedalling conditions. We selected muscles that contribute significantly to power production during cycling to explore how the functional role of these muscles might change with increases in torque and movement speed. Specifically, we used musculoskeletal simulations in combination with extensive experimental data on cycling to predict the functional roles of primary lower-limb muscles with increases in crank torque and pedalling cadence. We hypothesised that with greater crank torque at a constant speed, the mono-articular hip, knee and ankle extensors will generate greater positive muscle work and shift to an increasingly motor-like function. In contrast, the increasingly shorter cycle durations and earlier relative muscle activations in the same hip, knee and ankle extensors, as well as in bi-articular lower-limb muscles with faster pedalling cadence at a constant torque, will result in greater negative work and will cause the muscles to exhibit an increasingly spring-like (stretch–shorten) contractile function.

MATERIALS AND METHODS

Experimental protocol

Experimental data were collected from 20 competitive cyclists (10 male/10 female, mean±s.d. 30.6±7.3 years, 70.5±10.5 kg, 173.5±7.5 cm) as part of a comprehensive study of cycling across a range of pedalling conditions (Dick et al., 2017). Before participating, all subjects gave their informed consent and the study was approved by the ethics committees at Simon Fraser University and Harvard University.

Each cyclist underwent a cycling protocol where crank torque and pedalling cadence were varied independently for a total of eight pedalling conditions. The conditions included varied crank torque at a constant cadence of 80 rpm at 14, 26, 32 and 44 N m and varied cadence of 60, 100, 120 and 140 rpm at a constant crank torque of 13 N m. The average crank power output of each respective pedalling condition was 115, 220, 270, 370, 80, 135, 160 and 190 W. During each trial, 3D positions of 32 active LED markers placed on the pelvis, lower limbs and pedals were determined using a motion capture system sampling at 100 Hz (Certus Optotrak, NDI, Waterloo, ON, Canada). The specific marker locations are detailed in Dick et al. (2016). Normal and radial pedal reaction forces were measured bilaterally using clipless instrumented pedals sampling at 2000 Hz (Powerforce, Radlabor, Freiburg, Germany). The pedals were fixed to rigid, inflexible sandals worn by the cyclist. Electromyography (EMG) signals were recorded from 10 lower-limb muscles using bi-polar Ag/AgCl surface electrodes (20 mm inter-electrode distance) placed according to SENIEM guidelines and sampling at 2000 Hz (Biovision, Wehrheim, Germany). The lower-limb muscles recorded include the gluteus maximus (GMAX), rectus femoris (RF), biceps femoris long head (BF), semitendinosus (ST), vastus lateralis (VL), medial gastrocnemius (MG), lateral gastrocnemius (LG), soleus (SO) and tibialis anterior (TA). The information from the EMG signals was enhanced using a wavelet decomposition analysis, resolved over a range of frequency bands (6.9–395.44 Hz) to provide total EMG intensity for each muscle (Von Tscharner, 2000). The total EMG intensity represented the time-varying power of the signal with a time resolution of ∼20 ms for frequencies >100 Hz.

Musculoskeletal model

The musculoskeletal model used in this study represented the human lower limbs connected to bilateral pedals and a crank, totalling 18 segments and 26 degrees of freedom (dof) (Lai et al., 2017). The model was chosen because it was developed to investigate movements containing large amounts of hip and knee flexion, both of which occur during cycling. The pelvis had 6 dof and was free to translate and rotate in space, the hip had 3 rotational dof, the knee had 1 rotational dof with coupled tibiofemoral rotations and translations, the ankle–subtalar complex had 2 rotational dof, the pedal had 1 rotational dof, and the crank had 1 dof, which represented the crank angle. Finally, as a result of modelling constraints, the pedals were partitioned into two segments with a fixed constraint; one segment was fixed to the base of the foot and the other segment connected with 1 rotational dof to the crank. The mass and inertial properties of the upper limbs were lumped into the properties of the pelvis. Also, because of the rigidity in the sandals worn by the participants, the metatarsophalangeal joint was locked in the model.

The musculoskeletal model was driven by 80 massless Hill-type muscle–tendon unit (MTU) actuators. Each MTU represented a contractile element attached to a series elastic element (Millard et al., 2013). The contractile element was modelled with active force–length and force–velocity properties and passive force–length properties; the series elastic element was modelled with passive length–tension properties. Maximum shortening velocity was assumed to be 10 optimal fibre lengths per second (Zajac, 1989). Tendon compliance in the ankle plantarflexors and knee extensors

was set to 10% and 8% strain at maximum isometric force, respectively, which is consistent with the reported mechanical properties of the Achilles and patellar tendons (Kubo et al., 2001; Lichtwark and Wilson, 2005). Tendon compliance of all other lower-limb muscles was assumed to be 4.9% strain at maximum isometric force because of a lack of available experimental data (Millard et al., 2013).

Computational simulations

All computational simulations were performed in OpenSim (v.3.3; https://simtk.org/projects/opensim; Delp et al., 2007). The generic musculoskeletal model was scaled to the anthropometric dimensions to generate subject-specific models. The scaling tool used measurement-based scaling factors, obtained from the difference between the experimental and model markers of a static trial of the participant, to vary the mass and inertial properties as well as dimensions of the body segments. The subject-specific models were then used to compute joint angles and net joint torques around each dof using inverse kinematic and inverse dynamic tools, respectively. To obtain more dynamic consistency between the kinematics and the measured pedal reaction forces, a residual reduction algorithm (RRA) was used. During RRA, pelvis translation was fixed, which constrained the lower limbs to a closed loop between the crank and the pelvis. Constraining the pelvis assumes that residual forces were accumulated at the pelvis and transmitted out of the system through the seat. Residual torques at the pelvis were maintained. The kinematics obtained from RRA were input into a computed muscle control (CMC) algorithm, which used forward integration within a short time window (~0.015 s) to predict the muscle excitations, forces and energetics necessary to drive the computational simulations towards the measured kinematic trajectories (Thelen and Anderson, 2006; Thelen et al., 2003). In CMC, the cost function used to solve the force-sharing problem was to minimise the sum of muscle activations squared. The muscle excitations were bounded between 0 (no excitation) and 1 (full excitation). Across all simulations, the maximum root-mean-square errors for all pelvic rotations, pelvic translations and lower-limb dofs between the kinematics from RRA and CMC were on average 1.49 deg, 0.12 cm and 1.89 deg, respectively. For all successful simulations, reserve actuation at each dof was negligible compared with the muscle force contribution and was below the recommended maximum tolerance for CMC simulations (<25 N m; Hicks et al., 2015).

Mechanical work output and muscle function index

MTU mechanical power and work done were computed using instantaneous MTU force and MTU velocity. Power was calculated as the product of force and velocity while net positive and negative work done was calculated as the integral of the mechanical power with respect to time over a crank cycle. The mechanical force, power and work output for each muscle were used in a recently developed muscle functional index approach to characterise the primary function of the muscles during a given dynamic movement task (Lai et al., 2019). Briefly, the functional behaviour of a muscle was characterised into an index of four functions: motor-, spring-, strut- or damper-like. These functions were dimensionless and accumulated relative to each other up to 100%. In general, the muscle behaviour patterns were characterised by high values (>50%) of each index as follows: a high motor index is when a muscle performs predominantly net positive work; a high spring index is when negative and positive work are performed in approximately equal amounts, resulting in minimal net work; a high strut index is when high muscle force is coupled with isometric muscle behaviour, resulting in limited muscle work; and a high damper index is when a muscle performs predominantly negative work. For the indices to remain non-dimensional, a characteristic length factor was required that determined the influence of the strut index on the other three indices. This length factor was equivalent to the 1 rad angle factor used in the joint function index (Qiao and Jindrich, 2016). In our previous study, the length factor was determined using the assumption that the series elastic element acted in a predominantly spring-like manner during steady-state running. However, because we did not collect steady-state running dynamics for the participants in this study, we used the length factor of the MTU averaged across all the participants from a previous study (Lai et al., 2019) of steady-state running to characterise the functional index of the MTU.

Data analysis

For this study, the right leg was chosen for all cyclists as the leg of interest. Data were time normalised to crank time starting at top dead centre and used to calculate a group mean±s.d. In this study, we selected representative muscles that contributed at least 10% of the total net positive or negative work done during cycling and crossed the hip, knee and ankle joints. The selected muscles were the GMAX, BF, RF, VL, SO and TA. These uni- and bi-articular lower-limb muscles were also selected because they were largely unaffected by persistent passive force complications in the underlying 3D musculoskeletal model (Lai et al., 2017), which allowed their predicted muscle activation profiles to be consistent with the spatial and temporal profiles from the measured EMG intensities across pedalling conditions. Pearson coefficients were computed to compare the model-predicted and EMG-derived muscle activity profiles. EMG intensity and predicted activation were normalised to the peak intensity and activation, respectively, in each muscle across all the pedalling conditions.

To test our hypotheses, we performed multiple one-way repeated measures ANOVA using R (v.3.5) to test for statistical differences in output measures with respect to crank torque (4 levels: 14, 26, 32 and 44 N m at 80 rpm) and cadence (five levels: 60, 80, 100, 120 and 140 rpm at 13–14 N m). Output measures included total net positive and negative MTU work across the complete crank cycle as well as the ratio of spring-to-motor index and the strut index of each selected lower-limb muscle. The ratios of spring-to-motor index of each muscle were computed as the contribution of the spring index to the sum of the spring and motor indices. This ratio was chosen based on our hypotheses that increasing crank torque would induce more motor-like function and increasing cadence would induce more spring-like function. Statistical significance was set at $P<0.05$. MTU mechanical power and total net positive and negative MTU work done were normalised by body mass.

RESULTS

The spatial and temporal changes in both measured EMG intensity and model-predicted activation of lower-limb muscles across the boundary pedalling conditions of 80 rpm at 44 N m, 80 rpm at 14 N m and 140 rpm at 13 N m are shown in Fig. 1. On average, across all muscles and boundary conditions, the correlation between EMG intensity and model-predicted activation was 0.52, with highest correlation found for the VL (0.62), GMAX (0.89) and RF (0.56) across the three boundary conditions.

MTU positive power, generated by the GMAX, VL and SO, contributed a significant portion of the total mechanical power output in the sagittal plane. These MTU powers were coordinated during the downstroke phase of the crank cycle to transmit the mechanical power

Journal of Experimental Biology (2021) 224, jeb228221. doi:10.1242/jeb.228221

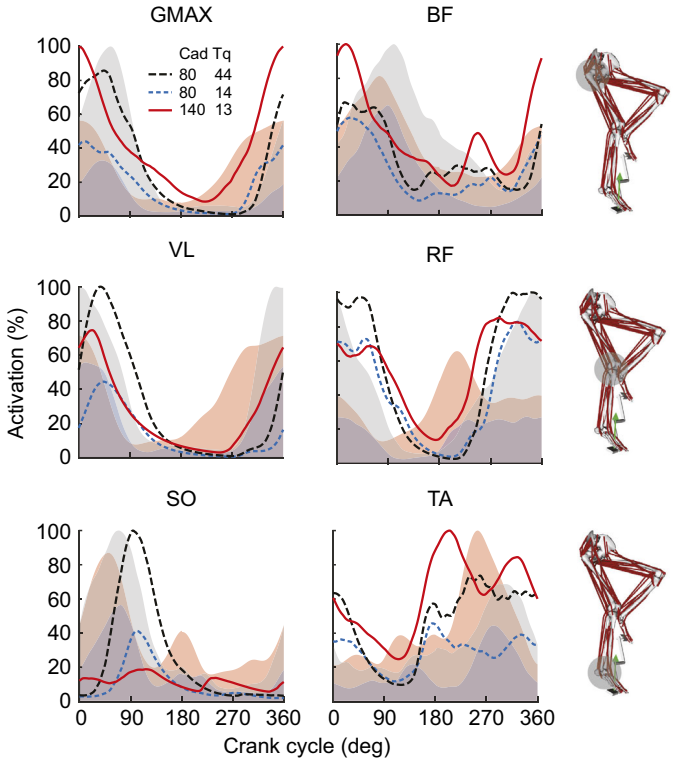

Fig. 1. EMG intensity (shading) and model-predicted muscle activation (lines) in the six selected lower-limb muscles across all cyclists during the three boundary pedalling conditions. The three boundary conditions were a pedalling cadence (Cad) and crank torque (Tq) of 80 rpm at 44 N m, 80 rpm at 14 N m and 140 rpm at 13 N m. EMG intensity and model-predicted activation were normalised to the peak intensity and activation, respectively, in each muscle across all the pedalling conditions. The selected lower-limb muscles include gluteus maximus (GMAX), biceps femoris (BF), vastus lateralis (VL), rectus femoris (RF), soleus (SO) and tibialis anterior (TA). The musculoskeletal model of the cyclist (right) denotes the primary joint spanned by the muscles based on their moment-generating capacity in the corresponding row.

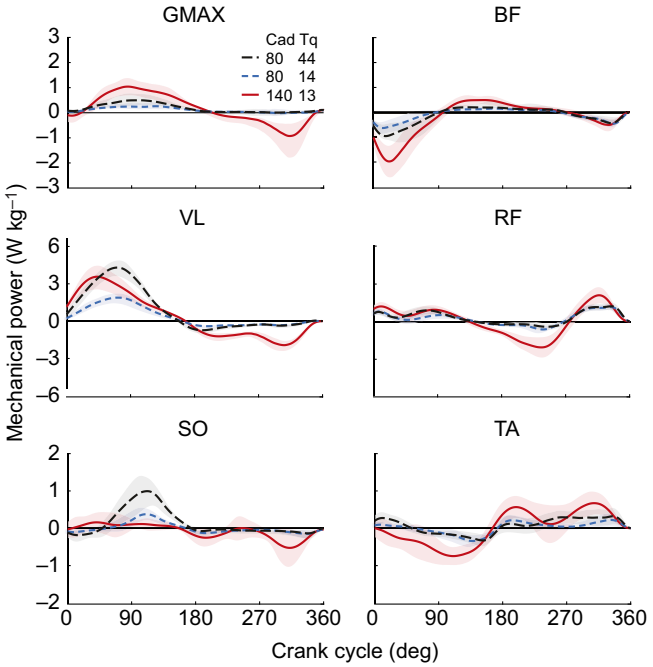

Fig. 2. Muscle–tendon unit (MTU) mechanical power for the six selected lower-limb muscles across all cyclists during three boundary pedalling conditions. The three boundary pedalling conditions were a pedalling cadence (Cad) and crank torque (Tq) of 80 rpm at 44 N m, 80 rpm at 14 N m and 140 rpm at 13 N m. Mechanical power was normalised to body mass. Lower-limb muscles include GMAX, BF, VL, RF, SO and TA.

to the crank through the foot–pedal interface (Fig. 2). Muscle coordination with greater crank torques from 13 N m to 44 N m at 80 rpm was particularly prominent in the VL and SO, and to a lesser extent in the GMAX, where these extensor muscles generated greater positive MTU power during the downstroke phase of the crank cycle. In the other lower-limb muscles that act primarily as flexors (i.e. RF, BF and TA), positive power output remained unchanged with increased crank torque. In contrast, all lower-limb muscles displayed a greater response to increases in pedalling cadence, particularly in generating greater negative MTU power. For example, during the upstroke phase of pedalling at 140 rpm at 13 N m, the GMAX, VL and RF generated greater negative MTU power compared with the other two 80 rpm pedalling conditions.

Total MTU work and contributions by the lower-limb muscles

Increases in crank torque and pedalling cadence significantly shifted total net, positive and negative MTU work done by the lower-limb muscles, as a whole (Fig. 3A). Specifically, total net MTU work significantly increased by ∼1.2 J kg^{-1} with greater crank torque from 14 N m to 44 N m at 80 rpm (P<0.001). These differences in the total net MTU work were a result of the significant changes in both total positive and total negative MTU work. In particular, with increased torque, total positive MTU work increased by ∼1.43 J kg^{-1} (P<0.001), whereby with increased cadence, total positive MTU work increased by ∼1.25 J kg^{-1} (P<0.001). Additionally, total negative MTU work was greater with increased torque from 14 N m to 44 N m at 80 rpm (−0.23 J kg^{-1}; P<0.001) and with increased cadence from 60 rpm to 140 rpm at 13 N m (−1.17 J kg^{-1}; P<0.001). Interestingly, the amount of total positive MTU work, 2.24±0.36 and 2.36±0.35 J kg^{-1}, was generated at an average crank power output of 80 rpm at 26 N m and 140 rpm at 13 N m, respectively, yet total net MTU work was less during a crank power output of 140 rpm at 13 N m because of the approximately −0.92 J kg^{-1} increase in total negative MTU work. The vastus muscle complex [VAS; consisting of the VL, vastus medialis (VMED) and vastus intermedius (VINT)] contributed the highest amount of net positive and negative MTU work of all lower-limb muscle groups (Fig. 3B–D). Specifically, across the pedalling conditions, the VAS contributed on average 47%, 31% and 19% of the total net positive and negative work, respectively. Given the important role of the VAS in cycling, the shifts in total MTU work with greater crank torque and faster pedalling cadence were associated with shifts in VAS MTU work. The RF and gluteus muscle complex [GL; consisting of the GMAX and gluteus medius (GMED)] were also key contributors to total MTU work, contributing 13% and −19% to total net MTU work, 13% and 10% to total positive MTU work, and 9% and 15% to total negative MTU work, respectively.

MTU functional roles with greater crank torque and faster pedalling cadence

In 5 of the 6 selected lower-limb muscles, the functional role of the MTUs shifted towards a more motor-like function to match the overall MTU mechanical power and work requirements with increases in crank torque (Figs 4 and 5). Specifically, we observed shifts in the contribution of the motor index and a

Journal of Experimental Biology (2021) 224, jeb228221. doi:10.1242/jeb.228221

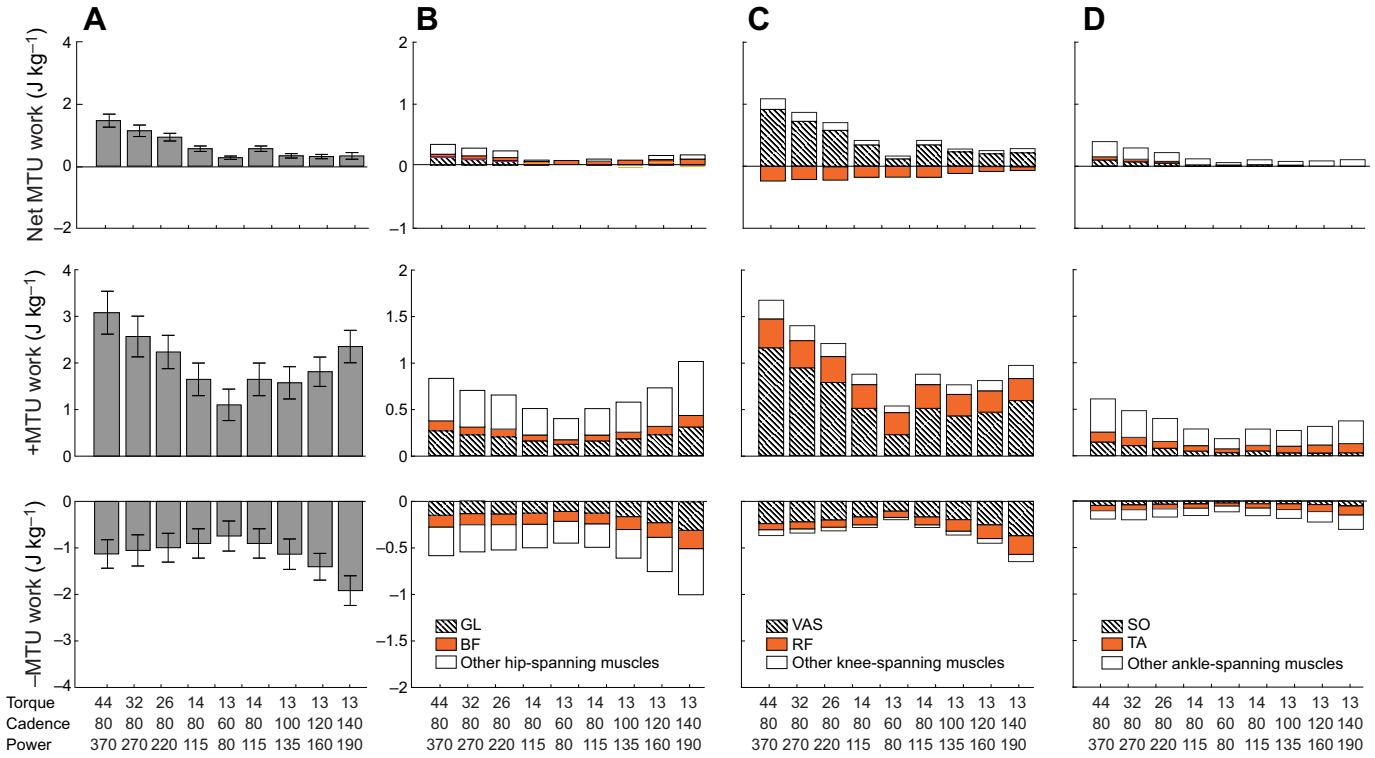

Fig. 3. Net (top), positive (middle) and negative (bottom) work done in the lower-limb muscles across all cyclists during all pedalling conditions. (A) Total MTU output of all the lower-limb muscles, (B) primary hip-spanning muscles, (C) primary knee-spanning muscles and (D) primary ankle-spanning muscles across eight pedalling conditions that varied crank torque and cadence. For simplicity, we combined the MTU work output of the vastus lateralis (VL), vastus medialis (VM) and vastus intermedius (VI) as a vastus muscle complex (VAS; C) and the gluteus maximus (GMAX) and gluteus medius (GMED) as a gluteus muscle complex (GL; B). MTU work was normalised by body mass. Other muscles represent the work done by muscles that were not included in the analysis of this study.

significant reduction in the spring-to-motor ratio in the GMAX, RF, VL, SO and TA with increases in torque (all $P<0.001$; Fig. 5). These shifts were most apparent in the VL and RF, for which during pedalling at 80 rpm at 44 N m, the differences between the motor to spring indices were 38% and 19%, for the VL and RF, respectively. These shifts coincided with increased EMG intensity and predicted activation in the corresponding muscles with greater crank torque (Fig. 1). Although significant shifts to greater motor-like function occurred for the GMAX, SO and TA, each MTU's spring index remained higher, particularly for the TA, in which the spring index averaged 60% across all pedalling conditions (Fig. 4).

In contrast to shifts in muscle function of the selected lower-limb muscles with greater crank torque, the majority of the muscles shifted their MTU functional role towards a more spring-like function with faster pedalling cadence (Figs 4 and 5). Specifically, we observed significant shifts in the contribution of the spring index to the spring-to-motor ratio in the GMAX ($P=0.002$), RF, VL, SO and TA (all $P<0.001$) (Fig. 5). Similar to the response of the muscles to greater crank torque, these shifts were most apparent in the VL and RF but also occurred in the GMAX and SO, with a difference between spring and motor indices of 53%, 72%, 67% and 32%, respectively, during pedalling at 140 rpm at 13 N m. The shift in the contribution of the spring index to the spring-to-motor ratio coincided with an average ∼70 deg earlier onset of EMG intensity and the predicted activation prior to pedal top dead centre in the corresponding muscles during the upstroke phase of pedalling (Fig. 1). In contrast, the functional role of the BF differed with respect to the other lower-limb muscles and exhibited a shift to a more spring-like function at the expense of damper- and strut-like function, instead of motor-like function ($P=0.12$), with increases in torque and cadence, respectively (Figs 4 and 5).

In addition to the spring, motor and damper indices, the strut index was high for the BF, RF and SO across pedalling conditions. Although no significant differences were found, the strut index was on average 31%, 32% and 68% in the BF, RF and SO, respectively, across crank torques at 80 rpm. However, with increased cadence, the strut index in the BF, RF and SO decreased significantly (all $P<0.001$); for example, by 33%, 27% and 17%, respectively, between 60 rpm and 140 rpm at 13 N m (Fig. 4). The shift in strut index was related to the increase in the spring-like function of these muscles. Yet, the SO functioned primarily in a strut-like way across pedalling conditions where, on average, the strut index was 64%.

DISCUSSION

The primary goal of cycling is to generate power and perform positive work with constrained lower-limb kinematics. Yet, within a seemingly simple task, muscles must adapt their function to satisfy changes in mechanical demands, which unlike weight-bearing tasks such as walking and running, can vary by independently increasing crank torque and movement speed (pedalling cadence). In this study, we combined experimental data of cycling with musculoskeletal simulations to examine whether the functions of different lower-limb muscles are sensitive to these changes in mechanical demands across a wide range of pedalling conditions. In support of our hypothesis, we found that for muscles that contribute to power production at the hip, knee and ankle during cycling (in particular the VL, SO and GMAX), greater crank torque induced shifts towards increased measured EMG intensity,

Journal of Experimental Biology (2021) 224, jeb228221. doi:10.1242/jeb.228221

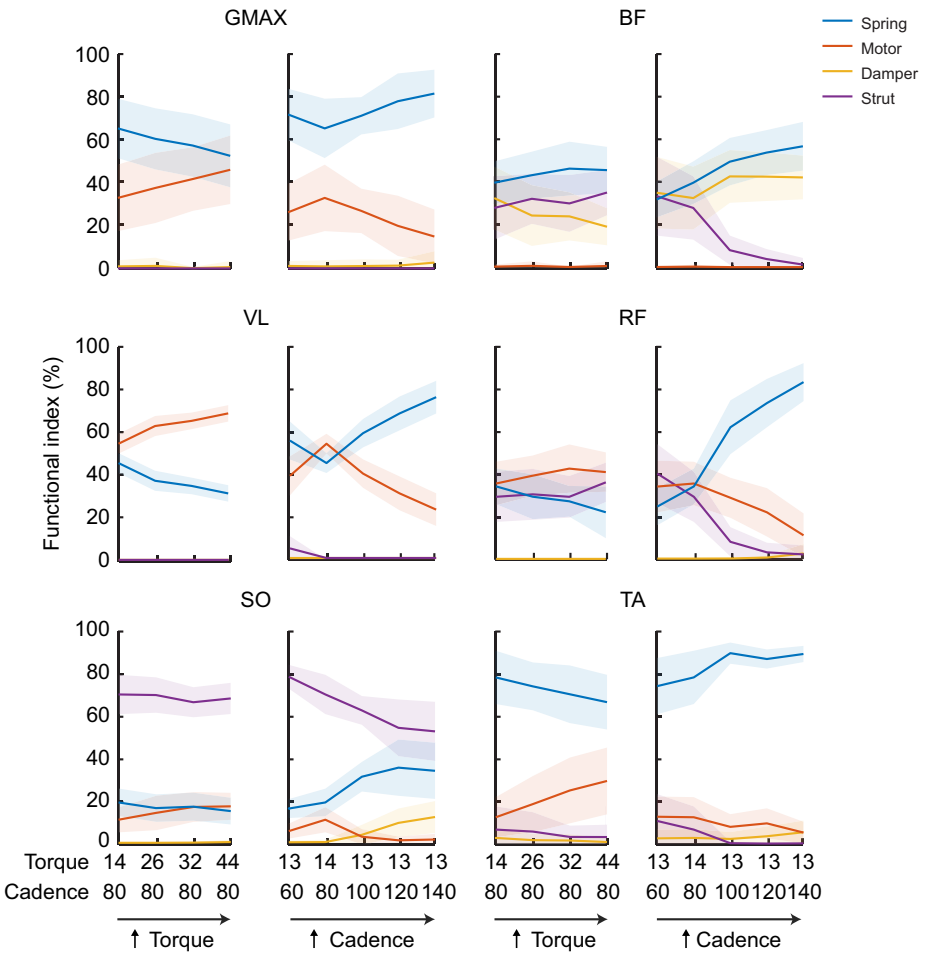

Fig. 4. Functional indices of the MTUs for the six selected lower-limb muscles across all cyclists and the eight pedalling conditions. The indices are dimensionless and were calculated relative to each other with a cumulative percentage of 100%. Lower-limb muscles include GMAX, BF, VL, RF, SO and TA.

increased predicted muscle activation, greater positive MTU power and work, and a more motor-like function. In contrast, with increased cadence, these same muscles exhibited a phase advance in muscle excitation prior to pedal top dead centre, which caused greater negative MTU power and work and shifted the muscles to a more spring-like function. These results illustrate the ability for MTUs to adapt their function to satisfy the mechanical demands of the task through their coordination of both the magnitude and timing of force and power production, even during a highly constrained reciprocal task such as cycling.

In the context of examining how the functional roles of human lower-limb MTUs vary with the changing mechanical demands of cycling, the function of each MTU involves underlying interactions between the muscle fibre and tendon components, each of which may differ from that of the whole MTU. MTU architecture has been shown to dictate interactions between the muscle fibre and tendon components, whereby in muscles, such as the SO and MG, a long, elastic tendon enables a spring-like behaviour as it stores and recovers a substantial amount of elastic strain energy during steady-state running (Lai et al., 2014). This muscle–tendon design, in turn,

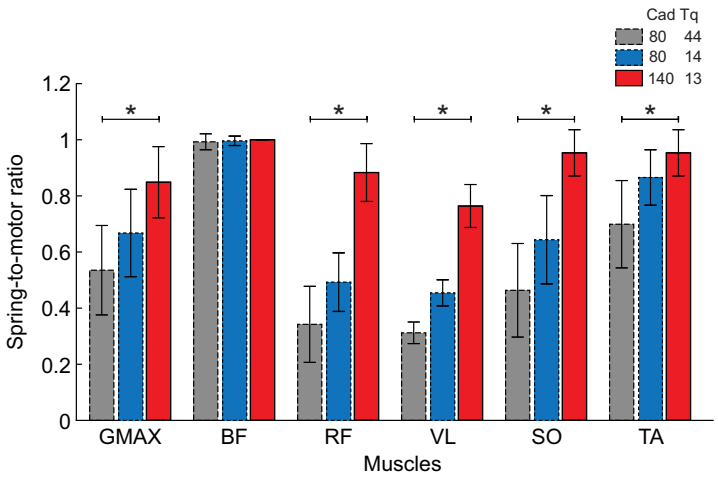

Fig. 5. The spring-to-motor ratio for the six selected lower-limb muscles across all cyclists during three boundary pedalling conditions. The ratio was calculated as the contribution of the spring index to the sum of the spring and motor indices. Asterisks denote statistical significance (*P<0.001). The three boundary pedalling conditions were a pedalling cadence (Cad) and crank torque (Tq) of 80 rpm at 44 N m, 80 rpm at 14 N m and 140 rpm at 13 N m. Lower-limb muscles include GMAX, BF, VL, RF, SO and TA. Note that larger spring-to-motor ratios reflect a change in muscle to a more spring-like behaviour and values greater than 0.5 are when spring-like behaviour was found to be greater than motor-like behaviour.

allows a more strut-like function of the muscle's fibres, which favours economical force development, but results in decoupling between the functional role of the muscle fibres and the whole MTU (Roberts and Azizi, 2011). In contrast, during the same movement, muscle fibre and MTU functions are more coupled in muscles with long, parallel muscle fibres and a much shorter tendon, such as GMAX. We observed that the time-varying strains of the muscle fibres were similar to those of their MTUs, irrespective of the muscle architecture. Hence, the shifts in MTU function with increased torque and cadence – required to propel a bike – were largely analogous to the function of the muscle fibres within the muscle, unlike previous observations of steady-state walking and running, for which MTU function reflected the role of the tendon (e.g. Lichtwark et al., 2007).

Although tendons are likely to be unable to store and recover substantial elastic strain energy during cycling, with faster cadences, the muscle fibres within the MTU increasingly undergo greater active lengthening to generate greater negative work (Neptune and Herzog, 1999), and this may assist the transfer of kinetic energy from the limb segments to the crank (Kautz and Neptune, 2002). The increase in negative MTU work is primarily due to the phase advance of muscle excitation prior to top dead centre during the upstroke phase of pedalling. Indeed, we observed an earlier onset of EMG intensity and predicted activation during the upstroke phase with increases in pedalling cadence in the GMAX, RF, BF and TA and particularly the VL (Fig. 1). Faster cadences reduce cycle duration and limit the time available for the muscles to deactivate prior to the subsequent crank cycle. In addition, muscles must control greater segmental accelerations with faster limb movement to maintain coordinated and smooth limb movement and to allow the higher segmental kinetic energy associated with higher segmental accelerations to be transferred to the crank to perform external work (Kautz and Neptune, 2002). As a result, the onset of muscle excitation is phase advanced with respect to top dead centre during the upstroke phase of pedalling to account for the time needed to activate and deactivate the muscle, as well as decelerate the limb and transfer energy to the crank (Fig. 1; Neptune et al., 1997; Wakeling and Horn, 2009). This earlier excitation and the greater proportion of activity for a given cycle duration results in greater active lengthening, increased negative MTU work and a more spring-like function, particularly for the VL, GMAX and RF (Figs 1 and 4).

The power profiles for these muscles were mirrored by similar profiles for the muscle fibres, suggesting that their increased spring-like function at higher cadences occurred at the level of the muscle fibres. A contributing candidate for increased spring-like capacity is the protein titin within these muscles. Titin has been proposed to increase the stiffness of a muscle when actively stretched (Herzog, 2014; Nishikawa et al., 2012; Rode et al., 2009), and recent genetic deletion experiments have supported the role of titin as a dynamically adaptable spring in the muscle (Monroy et al., 2017; Powers et al., 2016; Tahir et al., 2020). In our cycling experiments, it is possible that titin contributes to increased muscle stiffness when the muscle is actively lengthened, enabling titin to store more energy within the muscle at the end of the pedal cycle, and returning the energy in a spring-like manner at the beginning of the next cycle when the muscle fibres begin to shorten. This relationship was particularly notable for GMAX, which has been previously suggested as one of the hip extensor muscles that produces the majority of positive work during maximal cycling (Broker and Gregor, 1994; Martin and Brown, 2009). Yet, we show that GMAX can adapt and shift from primarily a motor-like function during pedalling at high crank torque to a more spring-like function with faster pedalling cadence, which cannot be inferred from joint dynamics and EMG activity alone.

Although the pedalling conditions of 80 rpm at 26 N m and 140 rpm at 13 N m generated approximately the same average crank power output (220 W versus 200 W, respectively; Dick et al., 2017) and joint kinematic trajectories, they exhibit distinctly different coordination patterns and muscle function profiles. We chose these conditions to decouple the effects of cadence from crank torque; however, it should be noted that because of the interaction between these parameters, maximal cycling at both high cadence and torque would probably incur a different set of muscle functions. During pedalling, muscles are required to accelerate and decelerate limb segments and produce crank torque (Kautz and Neptune, 2002). At very low crank torque and very high cadence, pedalling becomes a task associated more with segmental accelerations than producing crank torque. Comparing across the conditions in this study, the knee extensors, VL and RF exhibited the most noticeable differences in their functional roles where they primarily are motor-like during 80 rpm at 26 N m and spring-like during 140 rpm at 13 N m (Figs 4 and 5). This difference in function was due to the greater negative power and work generated primarily during the upstroke phase of the crank cycle during the faster cadence. This increase in negative power and work correlates with the phase advanced excitation of the RF and VL with shorter cycle durations, as noted above. These contrasting coordination patterns and muscle functions highlight the difference in strategy when increased crank power output is achieved through changes in either torque or cadence. With increased torque, power production and motor-like function are prioritised, while with increased cadence, timing of activity and coordination of the limbs that results in more spring-like function are prioritised. This prioritisation is consistent with recent findings that the variability in muscle coordination is reduced during pedalling at faster cadences (Hodson-Tole et al., 2019).

The RF, BF and SO all exhibited high strut-like function during pedalling, particularly during high crank torque conditions, suggesting that these muscles develop high force output with minimal MTU length change. As bi-articular muscles generate both hip and knee torques, the functions of the RF and BF during high torque conditions were consistent with their role in transferring energy between adjacent limb joints and controlling the direction of force development (Ryan and Gregor, 1992; van Ingen Schenau et al., 1992). In contrast, their behaviour shifted at faster pedalling cadences to a more spring-like function, which reflected the increased demand to coordinate the limbs and segmental accelerations rather than generating force and power. We expect that other bi-articular muscles, such as the medial and lateral gastrocnemii, which were not included here because of modelling limitations, would also exhibit similar shifts in function with changing demands during cycling.

The ability to determine the functional role of individual muscles based on the index-based approach employed in this study provides new insight to cycling research, which has previously been dominated by the perspective of the power- and work-producing roles of muscles during cycling. Lower-limb muscles do indeed produce substantial positive work, yet this is achieved in the context of also producing non-trivial negative work. This context was particularly evident during pedalling at higher cadences where five out of the six selected lower-limb muscles displayed a dominant spring-like function generating force during active lengthening and potentially returning some of this energy during the downstroke phase in conjunction with active shortening. It would therefore appear that in addition to positive work production, human muscles

during cycling adopt spring-like functions, probably to account for segmental accelerations (Kautz and Neptune, 2002), and do so by absorbing and generating minimal external energy.

A few limitations to this study should be acknowledged. First, there were temporal discrepancies between EMG intensity and predicted activation in the SO with increased cadence. These discrepancies were probably due to a combination of the use of mixed muscle properties to represent the fibre types within the SO, inaccuracies in the passive force properties of the underlying 3D musculoskeletal model, and the inability for simulations that use CMC and the predefined cost function in OpenSim to solve the force-sharing problem and predict co-contraction of antagonist muscle groups (Lai et al., 2017). The SO is composed of ∼90% slow-twitch and 10% fast-twitch muscle fibres (Johnson et al., 1973), which have different force-generating properties as well as activation dynamics. Yet, in our musculoskeletal simulations, we represented the SO with mixed properties, which most likely influenced the predicted activation in the SO at faster cadences where differences in maximum shortening velocity are significant. Second, the use of a single-element Hill-type muscle model has been shown to be unable to fully explain the different recruitment strategies that occur across mechanical demands (Lai et al., 2018). Third, other muscle-specific factors such as inertial properties and history-dependent effects were excluded from the muscle models (Ross et al., 2018). These exclusions, which limit the predictive accuracy of Hill-type models, probably influence the coordination, power, work and resulting function of the muscles across the examined pedalling conditions and, consequently, should be considered in future muscle-driven simulations. Despite this, the changing patterns in muscle function with the shifts in mechanical demands of cycling that our analysis reveal are generally insensitive to these exclusions because they were systematically applied across all simulations. In addition, the temporal and spatial changes in the predicted muscle activity in the selected muscles across the three boundary conditions were generally well correlated with EMG measured intensities, which further shows that the simulations in this study are feasible.

Finally, trained cyclists are capable of pedalling under conditions of higher torque and cadence than those examined here. While these conditions were not included, we propose that the relationships we report here would hold at higher torque and cadence, although with the increased power contributions from proximal muscles, as previously reported (Martin and Brown, 2009). For example, we would expect greater negative work done in the muscles with faster cadences, which may suggest that negative work limits the maximal cadence achievable by cyclists and influences the cadence that cyclists self-select. Last, we used an inverse-dynamics approach and experimental data to solve the force-sharing problem rather than predictive simulations that use approaches independent of experimental data, such as trajectory optimisation (Falisse et al., 2019). Although these approaches potentially provide greater insight into cause and effect relationships, the ability to define suitable objectives to achieve sub-maximal cycling across the range of mechanical demands and muscles is currently challenging and, even if achieved, may result in findings that are similar to results using more computationally effective methods (Anderson and Pandy, 2001).

In conclusion, using musculoskeletal simulations combined with non-invasive experimental data, we show that human lower-limb muscles can shift their functional role to meet broadly differing mechanical demands across the cycling conditions studied here. With increased torque, lower-limb MTUs shift towards a more motor-like function by increasing muscle activation and generating greater positive power and work. In contrast, with increased cadence, these lower-limb MTUs behave in a more spring-like way, with phase advanced muscle activation that generates greater negative power and work, followed by subsequent positive power and work.

Acknowledgements
We thank Allison Arnold and Sidney Morrison for their assistance in collecting and post-processing the experimental data used in this study.

Competing interests
The authors declare no competing or financial interests.

Author contributions
Conceptualization: A.K.M.L., T.J.M.D., A.A.B., J.M.W.; Methodology: A.K.M.L., T.J.M.D., A.A.B., J.M.W.; Software: A.K.M.L.; Validation: A.K.M.L.; Formal analysis: A.K.M.L.; Investigation: A.K.M.L., T.J.M.D., J.M.W.; Resources: A.K.M.L.; Data curation: A.K.M.L., T.J.M.D.; Writing - original draft: A.K.M.L., T.J.M.D., J.M.W.; Writing - review & editing: A.K.M.L., T.J.M.D., N.A.T.B., A.A.B., J.M.W.; Visualization: A.K.M.L.; Supervision: A.A.B., J.M.W.; Project administration: A.K.M.L., J.M.W.; Funding acquisition: A.A.B., J.M.W.

Funding
This study was financially supported by National Institutes of Health grant no. 2R01AR055648. Deposited in PMC for release after 12 months.

References
Anderson, F. C. and Pandy, M. G. (2001). Static and dynamic optimization solutions for gait are practically equivalent. *J. Biomech.* **34**, 153-161. doi:10.1016/S0021-9290(00)00155-X

Biewener, A. A. (1998). Muscle function in vivo: a comparison of muscles used for elastic energy savings versus muscles used to generate mechanical power. *Am. Zool.* **38**, 703-717. doi:10.1093/icb/38.4.703

Biewener, A. A., McGowan, C., Card, G. M. and Baudinette, R. V. (2004). Dynamics of leg muscle function in tammar wallabies (M. eugenii) during level versus incline hopping. *J. Exp. Biol.* **207**, 211-223. doi:10.1242/jeb.00764

Broker, J. P. and Gregor, R. J. (1994). Mechanical energy management in cycling: source relations and energy expenditure. *Med. Sci. Sports Exerc.* **26**, 64-74. doi:10.1249/00005768-199401000-00012

Daley, M. A. and Biewener, A. A. (2003). Muscle force-length dynamics during level versus incline locomotion: a comparison of in vivo performance of two guinea fowl ankle extensors. *J. Exp. Biol.* **206**, 2941-2958. doi:10.1242/jeb.00503

Delp, S. L., Anderson, F. C., Arnold, A. S., Loan, P., Habib, A., John, C. T., Guendelman, E. and Thelen, D. G. (2007). OpenSim: Open-source software to create and analyze dynamic simulations of movement. *IEEE Trans. Biomed. Eng.* **54**, 1940-1950. doi:10.1109/TBME.2007.901024

Dick, T. J. M., Arnold, A. S. and Wakeling, J. M. (2016). Quantifying Achilles tendon force in vivo from ultrasound images. *J. Biomech.* **49**, 3200-3207. doi:10.1016/j.jbiomech.2016.07.036

Dick, T. J. M., Biewener, A. A. and Wakeling, J. M. (2017). Comparison of human gastrocnemius forces predicted by Hill-type muscle models and estimated from ultrasound images. *J. Exp. Biol.* **220**, 1643-1653. doi:10.1242/jeb.154807

Dickinson, M. H., Farley, C. T., Full, R. J., Koehl, M. A., Kram, R. and Lehman, S. (2000). How animals move: An integrative view. *Science (80-.).* **288**, 100-106. doi:10.1126/science.288.5463.100

Ericson, M. O. (1988). Mechanical muscular power output and work during ergometer cycling at different work loads and speeds. *Eur. J. Appl. Physiol. Occup. Physiol.* **57**, 382-387. doi:10.1007/BF00417980

Falisse, A., Serrancolí, G., Dembia, C. L., Gillis, J., Jonkers, I. and De Groote, F. (2019). Rapid predictive simulations with complex musculoskeletal models suggest that diverse healthy and pathological human gaits can emerge from similar control strategies. *J. R. Soc. Interface* **16**, 20190402. doi:10.1098/rsif.2019.0402

Herzog, W. (2014). The role of titin in eccentric muscle contraction. *J. Exp. Biol.* **217**, 2825-2833. doi:10.1242/jeb.099127

Hicks, J. L., Uchida, T. K., Seth, A., Rajagopal, A. and Delp, S. L. (2015). Is my model good enough? Best practices for verification and validation of musculoskeletal models and simulations of movement. *J. Biomech. Eng.* **137**, 1-24. doi:10.1115/1.4029304

Hodson-Tole, E. F., Blake, O. M. and Wakeling, J. M. (2019). During cycling what limits maximum mechanical power output at cadences above 120 rpm? *Med. Sci. Sports Exerc* **52**, 214-224. doi:10.1249/MSS.0000000000002096

Hug, F. and Dorel, S. (2009). Electromyographic analysis of pedaling: a review. *J. Electromyogr. Kinesiol.* **19**, 182-198. doi:10.1016/j.jelekin.2007.10.010

Hull, M. L. and Jorge, M. (1985). A method for biomechanical analysis of bicycle pedalling. *J. Biomech.* **18**, 631-644. doi:10.1016/0021-9290(85)90019-3
Johnson, M. A., Polgar, J., Weightman, D. and Appleton, D. (1973). Data on the distribution of fibre types in thirty-six human muscles. *An autopsy study. J. Neurol. Sci.* **18**, 111-129. doi:10.1016/0022-510X(73)90023-3
Josephson, R. K. (1985). Mechanical power output from striated muscle during cyclic contraction. *J. Exp. Biol.* **114**, 493-512.
Katz, S. L., Syme, D. A. and Shadwick, R. E. (2001). High-speed swimming: enhanced power in yellowfin tuna. *Nature* **410**, 770-771. doi:10.1038/35071170
Kautz, S. A. and Neptune, R. R. (2002). Biomechanical determinants of pedaling energetics: internal and external work are not independent. *Exerc. Sport Sci. Rev.* **30**, 159-165. doi:10.1097/00003677-200210000-00004
Kubo, K., Kanehisa, H. and Ito, M. (2001). Effects of isometric training on the elasticity of human tendon structures in vivo. *J. Appl. Physiol.* **91**, 26-32. doi:10.1152/jappl.2001.91.1.26
Lai, A., Schache, A. G., Lin, Y.-C. and Pandy, M. G. (2014). Tendon elastic strain energy in the human ankle plantar-flexors and its role with increased running speed. *J. Exp. Biol.* **217**, 3159-3168. doi:10.1242/jeb.100826
Lai, A. K. M., Arnold, A. S. and Wakeling, J. M. (2017). Why are antagonist muscles co-activated in my simulation? A musculoskeletal model for analysing human locomotor tasks. *Ann. Biomed. Eng.* **45**, 2762-2774. doi:10.1007/s10439-017-1920-7
Lai, A. K. M., Biewener, A. A. and Wakeling, J. M. (2018). Metabolic cost underlies task-dependent variations in motor unit recruitment. *J. R. Soc. Interface* **15**, 20180541. doi:10.1098/rsif.2018.0541
Lai, A. K. M., Biewener, A. A. and Wakeling, J. M. (2019). Muscle-specific indices to characterise the functional behaviour of human lower-limb muscles during locomotion. *J. Biomech.* **89**, 134-138. doi:10.1016/j.jbiomech.2019.04.027
Lichtwark, G. A. and Wilson, A. M. (2005). In vivo mechanical properties of the human Achilles tendon during one-legged hopping. *J. Exp. Biol.* **208**, 4715-4725. doi:10.1242/jeb.01950
Lichtwark, G. A., Bougoulias, K. and Wilson, A. M. (2007). Muscle fascicle and series elastic element length changes along the length of the human gastrocnemius during walking and running. *J. Biomech.* **40**, 157-164. doi:10.1016/j.jbiomech.2005.10.035
Martin, J. C. and Brown, N. A. T. (2009). Joint-specific power production and fatigue during maximal cycling. *J. Biomech.* **42**, 474-479. doi:10.1016/j.jbiomech.2008.11.015
Martin, J. C. and Nichols, J. A. (2018). Simulated work loops predict maximal human cycling power. *J. Exp. Biol.* **221**, jeb180109. doi:10.1242/jeb.180109
Millard, M., Uchida, T., Seth, A. and Delp, S. L. (2013). Flexing computational muscle: modeling and simulation of musculotendon dynamics. *J. Biomech. Eng.* **135**, 1-11. doi:10.1115/1.4023390
Monroy, J. A., Powers, K. L., Pace, C. M., Uyeno, T. and Nishikawa, K. C. (2017). Effects of activation on the elastic properties of intact soleus muscles with a deletion in titin. *J. Exp. Biol.* **220**, 828-836. doi:10.1242/jeb.139717
Neptune, R. R. and Herzog, W. (1999). The association between negative muscle work and pedaling rate. *J. Biomech.* **32**, 1021-1026. doi:10.1016/S0021-9290(99)00100-1
Neptune, R. R. and van den Bogert, A. J. (1997). Standard mechanical energy analyses do not correlate with muscle work in cycling. *J. Biomech.* **31**, 239-245. doi:10.1016/S0021-9290(97)00129-2
Neptune, R. R., Kautz, S. A. and Hull, M. L. (1997). The effect of pedaling rate on coordination in cycling. *J. Biomech.* **30**, 1051-1058. doi:10.1016/S0021-9290(97)00071-7
Nishikawa, K. C., Monroy, J. A., Uyeno, T. E., Yeo, S. H., Pai, D. K. and Lindstedt, S. L. (2012). Is titin a "winding filament"? A new twist on muscle contraction. *Proc. R. Soc. B Biol. Sci.* **279**, 981-990. doi:10.1098/rspb.2011.1304
Powers, K., Nishikawa, K., Joumaa, V. and Herzog, W. (2016). Decreased force enhancement in skeletal muscle sarcomeres with a deletion in titin. *J. Exp. Biol.* **219**, 1311-1316. doi:10.1242/jeb.132027
Qiao, M. and Jindrich, D. L. (2016). Leg joint function during walking acceleration and deceleration. *J. Biomech.* **49**, 66-72. doi:10.1016/j.jbiomech.2015.11.022
Roberts, T. J. and Azizi, E. (2011). Flexible mechanisms: the diverse roles of biological springs in vertebrate movement. *J. Exp. Biol.* **214**, 353-361. doi:10.1242/jeb.038588
Roberts, T. J., Marsh, R. L., Weyand, P. G. and Taylor, C. R. (1997). Muscular force in running turkeys: the economy of minimizing work. *Science (80-.)* **275**, 1113-1115. doi:10.1126/science.275.5303.1113
Rode, C., Siebert, T. and Blickhan, R. (2009). Titin-induced force enhancement and force depression: a "sticky-spring" mechanism in muscle contractions? *J. Theor. Biol.* **259**, 350-360. doi:10.1016/j.jtbi.2009.03.015
Ross, S. A., Ryan, D. S., Dominguez, S., Nigam, N. and Wakeling, J. M. (2018). Size, history-dependent, activation and three-dimensional effects on the work and power produced during cyclic muscle contractions. *Integr. Comp. Biol.* **58**, 232-250. doi:10.1093/icb/icy021
Ryan, M. M. and Gregor, R. J. (1992). EMG profiles of lower extremity muscles during cycling at constant workload and cadence. *J. Electromyogr. Kinesiol.* **2**, 69-80. doi:10.1016/1050-6411(92)90018-E
Tahir, U., Monroy, J. A., Rice, N. A. and Nishikawa, K. C. (2020). Effects of a titin mutation on force enhancement and force depression in mouse soleus muscles. *J. Exp. Biol.* **223**, jeb197038. doi:10.1242/jeb.197038
Thelen, D. G. and Anderson, F. C. (2006). Using computed muscle control to generate forward dynamic simulations of human walking from experimental data. *J. Biomech.* **39**, 1107-1115. doi:10.1016/j.jbiomech.2005.02.010
Thelen, D. G., Anderson, F. C. and Delp, S. L. (2003). Generating dynamic simulations of movement using computed muscle control. *J. Biomech.* **36**, 321-328. doi:10.1016/S0021-9290(02)00432-3
van Ingen Schenau, G. J., Boots, P. J. M., de Groot, G., Snackers, R. J. and van Woensel, W. W. L. M. (1992). The constrained control of force and position in multi-joint movements. *Neuroscience* **46**, 197-207. doi:10.1016/0306-4522(92)90019-X
Von Tscharner, V. (2000). Intensity analysis in time-frequency space of surface myoelectric signals by wavelets of specified resolution. *J. Electromyogr. Kinesiol.* **10**, 433-445. doi:10.1016/S1050-6411(00)00030-4
Wakeling, J. M. and Horn, T. (2009). Neuromechanics of muscle synergies during cycling. *J. Neurophysiol.* **101**, 843-854. doi:10.1152/jn.90679.2008
Zajac, F. E. (1989). Muscle and tendon: properties, models, scaling, and application to biomechanics and motor control. *Crit. Rev. Biomed. Eng.* **17**, 359-411.